THE JOURNAL OF BIOLOGICAL CHEMISTRY Vol. 278, No. 28, Issue of July 11, pp. 25468–25480, 2003

Printed in U.S.A.

The Human Apolipoprotein AV Gene Is Regulated by Peroxisome Proliferator-activated Receptor-α and Contains a Novel Farnesoid X-activated Receptor Response Element*

Received for publication, February 6, 2003, and in revised form, March 21, 2003
Published, JBC Papers in Press, April 22, 2003, DOI 10.1074/jbc.M301302200

Xavier Prieur, Hervé Coste, and Joan C. Rodríguez‡

From GlaxoSmithKline, 25 Avenue du Québec, 91951 Les Ulis cedex, France

The newly identified apolipoprotein AV (apoAV) gene is a key player in determining plasma triglyceride concentrations. Because hypertriglyceridemia is a major independent risk factor in coronary artery disease, the understanding of the regulation of the expression of this gene is of considerable importance. We presently characterize the structure, the transcription start site, and the promoter of the human apoAV gene. Since the peroxisome proliferator-activated receptor-α (PPARα) and the farnesoid X-activated receptor (FXR) have been shown to modulate the expression of genes involved in triglyceride metabolism, we evaluated the potential role of these nuclear receptors in the regulation of apoAV transcription. Bile acids and FXR induced the apoAV gene promoter activity. 5′-Deletion, mutagenesis, and gel shift analysis identified a heretofore unknown element at positions −103/−84 consisting of an inverted repeat of two consensus receptor-binding hexads separated by 8 nucleotides (IR8), which was required for the response to bile acid-activated FXR. The isolated IR8 element conferred FXR responsiveness on a heterologous promoter. On the other hand, in apoAV-expressing human hepatic Hep3B cells, transfection of PPARα specifically enhanced apoAV promoter activity. By deletion, site-directed mutagenesis, and binding analysis, a PPARα response element located 271 bp upstream of the transcription start site was identified. Finally, treatment with a specific PPARα activator led to a significant induction of apoAV mRNA expression in hepatocytes. The identification of apoAV as a PPARα target gene has major implications with respect to mechanisms whereby pharmacological PPARα agonists may exert their beneficial hypotriglyceridemic actions.

Recent epidemiological studies have shown that hypertriglyceridemia is a major independent risk factor for coronary heart disease, which remains as a major cause of mortality in the Western world (1–6). Understanding the factors that control plasma triglyceride levels and the genes that primarily reflect circulating concentrations of triglyceride-rich lipoproteins is thus of major importance and may provide new opportunities for therapeutic intervention in atherogenic dyslipidemia.

Pharmacological activation of peroxisome proliferator-activated receptor-α (PPARα[1]; NR1C1) lowers plasma levels of triglyceride-rich lipoproteins markedly (7, 8). PPARα is a fatty acid-activated nuclear transcription factor that regulates the expression of genes involved in lipid and energy metabolism (9, 10). PPARα heterodimerizes with the retinoid X receptor α (RXRα; NR2B1) and binds to specific DNA sequence elements, designated PPREs, which consist of a direct repeat of the hexanucleotide core motif PuGGTCA separated by 1 or 2 nucleotides (DR1 or DR2). PPARα mediates the hypotriglyceridemic effect of fibrates by regulating the transcription of key genes associated with different intra- and extracellular metabolic pathways. Fibrates increase cellular fatty acid transport and uptake, conversion to acyl-CoA derivatives, and catabolism by β-oxidation, which results in decreased substrate availability for triglyceride synthesis and very low density lipoprotein production by the liver. In addition, activated PPARα promotes lipolysis and clearance of triglyceride-rich lipoproteins, thus decreasing the plasma levels of triglycerides (11). These extracellular effects have been attributed to an increase in LPL activity via induction of its expression in the liver and reduction of hepatic expression (and subsequently serum levels) of apolipoprotein CIII (apoCIII), an established inhibitor of LPL activity and remnant particle catabolism (7, 12–15).

The farnesoid X-activated receptor (FXR, NR1H4) is another member of the nuclear receptor superfamily that has been described as a key regulator in the control of plasma triglyceride levels (16). The expression of FXR is restricted to the liver, intestine, kidney, and adrenal cortex (17, 18). FXR is a bile acid-activated receptor that alters transcription by binding as a heterodimer with RXR to response elements (FXREs) within the regulatory regions of target genes (16–21). With two exceptions, FXREs consist of an inverted repeat of the canonical hexanucleotide core motif PuGGTCA spaced by one base pair (IR1) (16). Recently, an inverted repeat with no spacer (IR0) in the dehydroepiandrosterone sulfotransferase gene (22) and an everted repeat of the core motif separated by 8 nucleotides (ER8) in the multidrug resistance-associated protein 2 (MRP2)

* This work was supported by a Marie Curie Fellowship of the European Community program Quality of Life under contract number QLK5-CT-2000-60009. The costs of publication of this article were defrayed in part by the payment of page charges. This article must therefore be hereby marked "*advertisement*" in accordance with 18 U.S.C. Section 1734 solely to indicate this fact.

‡ To whom correspondence should be addressed. Tel.: 33-1-69-29-61-22; Fax: 33-1-69-07-48-92; E-mail: jcrodrig@freesurf.fr.

[1] The abbreviations and trivial name used are: PPARα, peroxisome proliferator-activated receptor α; apoAI, apoAIV, apoAV, apoCII, and apoCIII, apolipoprotein AI, AIV, AV, CII, and CIII, respectively; CDCA, chenodeoxycholic acid; DR, direct repeat; FXR, farnesoid X-activated receptor; ER, everted repeat; FXRE, farnesoid X-activated receptor response element; I-BABP, ileal-bile acid-binding protein; IR, inverted repeat; LCA, lithocholic acid; LPL, lipoprotein lipase; mitHMGS, mitochondrial 3-hydroxy-3-methylglutaryl-CoA synthase; MRP2, multidrug resistance-associated protein 2; nt, nucleotide(s); PPRE, peroxisome proliferator-activated receptor response element; RACE, rapid amplification of cDNA ends; RLM-RACE, RNA ligase-mediated RACE; RT-PCR, reverse transcriptase-PCR; RXRα, retinoid X receptor α; SNP, single nucleotide polymorphism; TK, thymidine kinase; FCS, fetal calf serum; GW9003, propanoic acid, 2-[4-[[[[2-(4-chlorophenyl)-4-methyl-5-thiazolyl]carbonyl] amino]methyl]phenoxy]-2-methyl-(9Cl).

TABLE I
Primers used in this study

Mutated nucleotides are denoted in *boldface* and *lowercase* type.

Name		Sequence (5′ → 3′)	Use in this study
JCR 81	hapoAV ex 4 AS	GATCCATCGTGTAGGGCTTCAGTTG	RLM-RACE
JCR 80	hapoAV ex 4 AS	ATGTAGGGCTGGAGGCGAGCCTTCAC	RLM-RACE
JCR 79	hapoAV ex 4 AS	AGAGGCCTCAGCTTTTCCAGGAACTTG	RLM-RACE
JCR 65	hapoAV −2455 F	AGTCGGTACCTCAACTGGGCTTGCCCTATGC	Transfections
JCR 44	hapoAV −617 C F	AGTCGGTACCTCATGGGGCAAATCTCACTTTCGC	Transfections
JCR 45	hapoAV −617 T F	AGTCGGTACCTCATGGGGCAAATCTTACTTTCGC	Transfections
JCR107	hapoAV −535 F	AGTCGGTACCCTGCCTGGCTTCCCTTGCTTG	Transfections
JCR108	hapoAV −437 F	AGTCGGTACCTGTAGTGAAGCTTTCAGG	Transfections
JCR109	hapoAV −242 F	AGTCGGTACCTGGGTGAGGAGTTCAGCCCCATCC	Transfections
JCR110	hapoAV −82 F	AGTCGGTACCACGTGGTATTTACTCAGAGC	Transfections
JCR 95	hapoAV +18 R	AGTCGCTAGCTCACCTGCTCACGTCTGG	Transfections
JCR 96	hapoAV +529 R	AGTCGCTAGCCTGCTCTGAGAAGACAGG	Transfections
JCR 117	hapoAV −617/−593 F	GATCCTCATGGGGCAAATCTCACTTTCGA	EMSA
JCR 118	hapoAV −617/−593 R	GATCTCGAAAGTGAGATTTGCCCCATGAG	EMSA
JCR 141	hapoAV −275/−247 F	GATCCGGGAAGGTTAAAGGTCATGGGGTTTGGGA	EMSA
JCR 142	hapoAV −275/−247 R	GATCTCCCAAACCCCATGACCTTTAACCTTCCCG	EMSA
JCR 155	hapoAV −169/−147 F	GATCCAGGGCACTCATTAACCCTCTGA	EMSA
JCR 156	hapoAV −169/−147 R	GATCTCAGAGGGTTAATGAGTGCCCTG	EMSA
JCR 153	hapoAV −144/−117 F	GATCCTGCCAGGGAAAGGGCAGGAGGTGAGTGCA	EMSA
JCR 154	hapoAV −144/−117 R	GATCTGCACTCACCTCCTGCCCTTTCCCTGGCAG	EMSA
JCR 151	hapoAV −52/−31 F	GATCCAGAGGCTCAGGGCCCTGGAGA	EMSA
JCR 152	hapoAV −52/−31 R	GATCTCTCCAGGGCCCTGAGCCTCTG	EMSA
JCR 157	mitHMGS −113/−82 F	GATCCTTGTTCTGAGACCTTTGGCCCAGTTTTTCTGA	EMSA
JCR 158	mitHMGS −113/−82 R	GATCTCAGAAAAACTGGGCCAAAGGTCTCAGAACAAG	EMSA
JCR 145	hapoAV −484/−462 F	GATCCGTGGTTGGTCTTTAACCCTATGA	EMSA
JCR 146	hapoAV −484/−462 R	GATCTCATAGGGTTAAAGACCAACCACG	EMSA
JCR 123	hapoAV −399/−374 F	GATCCTGGTAGGTGAACACTGTCCATCTTGA	EMSA
JCR 124	hapoAV −399/−374 R	GATCTCAAGATGGACAGTGTTCACCTACCAG	EMSA
JCR 143	hapoAV −298/−263 F	GATCCGGTGGGCCAGCCAGCAGGTCAGTGGGAAGGTTAAAGA	EMSA
JCR 144	hapoAV −298/−263 R	GATCTCTTTAACCTTCCCACTGACCTGCTGGCTGGCCCACCG	EMSA
JCR 165	hapoAV mt DR1 F	GATCCGGGAAGGTTAAA**caa**CATGGGGTTTGGGA	EMSA
JCR 166	hapoAV mt DR1 R	GATCTCCCAAACCCCATG**ttg**TTTAACCTTCCCG	EMSA
JCR 147	hI-BABP FXRE F	GATCCCAGGGTGAATAACCTCGGGGA	EMSA
JCR 148	hI-BABP FXRE R	GATCTCCCCGAGGTTATTCACCCTGG	EMSA
JCR 169	hapoAV dirmut DR1 F	GCAGGTCAGTGGGAAGGTTAAA**caa**CATGGGGTTTGGGAG	Site-directed mutagenesis
JCR 170	hapoAV dirmut DR1 R	CTCCCAAACCCCATG**ttg**TTTAACCTTCCCACTGACCTGC	Site-directed mutagenesis
JCR 167	hapoAV dirmut IR8 F	GCTGGGAGGCAGCTGAG**aa**CAACTTCTTTcGttCTTCCACGTGG	Site-directed mutagenesis
JCR 168	hapoAV dirmut IR8 R	CCACGTGGAAG**aa**CgAAAGAAGTTG**tt**CTCAGCTGCCTCCCAGC	Site-directed mutagenesis
JCR 139	hapoAV −109/−80 F	GATCCAGCTGAGGTCAACTTCTTTTGAACTTCCA	Transfections and EMSA
JCR 140	hapoAV −109/−80 R	GATCTGGAAGTTCAAAAGAAGTTGACCTCAGCTG	Transfections and EMSA
JCR 159	hapoAV mt1 IR8 F	GATCCAGCTGAG**aa**CAACTTCTTTTGAACTTCCA	Transfections and EMSA
JCR 160	hapoAV mt1 IR8 R	GATCTGGAAGTTCAAAAGAAGTTG**tt**CTCAGCTG	Transfections and EMSA
JCR 161	hapoAV mt2 IR8 F	GATCCAGCTGAGGTCAACTTCTTT**cG**t**t**CTTCCA	Transfections and EMSA
JCR 162	hapoAV mt2 IR8 R	GATCTGGAAG**aa**CgAAAGAAGTTGACCTCAGCTG	Transfections and EMSA
JCR 163	hapoAV mt3 IR8 F	GATCCAGCTGAG**aa**CAACTTCTTT**cG**t**t**CTTCCA	Transfections and EMSA
JCR 164	hapoAV mt3 IR8 R	GATCTGGAAG**aaCg**AAAGAAGTTG**tt**CTCAGCTG	Transfections and EMSA
JCR36	18 S S	GGGAGCCTGAGAAACGGC	Real time RT-PCR
JCR37	18 S AS	GGGTCGGGAGTGGGTAATTT	Real time RT-PCR
XP3	hapoAV S	AGCTGGTGGGCTGGAATTT	Real time RT-PCR
XP4	hapoAV AS	GGCCACCTGCTCCATCAG	Real time RT-PCR
BA1	hBSEP S	GGTGAGAAAAGAGAGGTTGAAAGG	Real time RT-PCR
BA2	hBSEP AS	CCACACGAATCCAGTAAAGAATCC	Real time RT-PCR
BA3	hSHP S	CGCCCTATCATTGGAGATGT	Real time RT-PCR
BA4	hSHP AS	AGGAGCATTGGGTCACCTC	Real time RT-PCR

gene (23) have also been reported as elements required for FXR-dependent transcriptional activation. FXR acts as a bile acid sensor in the liver, where it mediates the negative feedback of bile acid biosynthesis via induction of small heterodimer partner (NR0B2) and subsequent repression of cholesterol 7α-hydroxylase gene (*CYP7A1*) expression (24–27), the rate-limiting enzyme in this pathway, and the sterol 12α-hydroxylase gene (*CYP8B1*), the specific enzyme required for cholic acid synthesis (28). FXR also controls the transport of bile acids in the liver and intestine. It promotes the excretion of bile acids from hepatocytes into the bile by induction of bile salt export pump gene expression (29) and stimulates the enterohepatic circulation of bile acids by activation of the transcription of ileal-bile acid-binding protein (I-BABP) (30). In addition, recent findings have shown that FXR regulates lipoprotein metabolism (16). Phospholipid transfer protein and apoAI, two major players in plasma high density lipoprotein metabolism, have been described as FXR target genes (31–33). Studies in rodents have revealed the role of FXR in regulating triglyceride levels. The administration of either a synthetic FXR ligand (GW4064) (34) or a natural FXR ligand (cholic acid) (35) to rodents resulted in at least a 50% decrease in plasma triglyceride levels. Consistent with these observations, FXR-deficient mice exhibited a 150% increase in plasma triglyceride levels (36). Importantly, Edwards and co-workers (35) have reported that activated FXR induces the expression of apoCII, an obligate cofactor for LPL, which in turn would result in the hydrolysis of triglycerides in chylomicrons and very low density lipoprotein. These data provide a mechanism to explain the hypotriglyceridemic effects of the natural FXR activator chenodeoxycholic acid (CDCA) when administered to patients with cholesterol-rich gallstones (37).

Recently, a novel apolipoprotein, designated apoAV, was suggested to play a significant role on plasma triglyceride

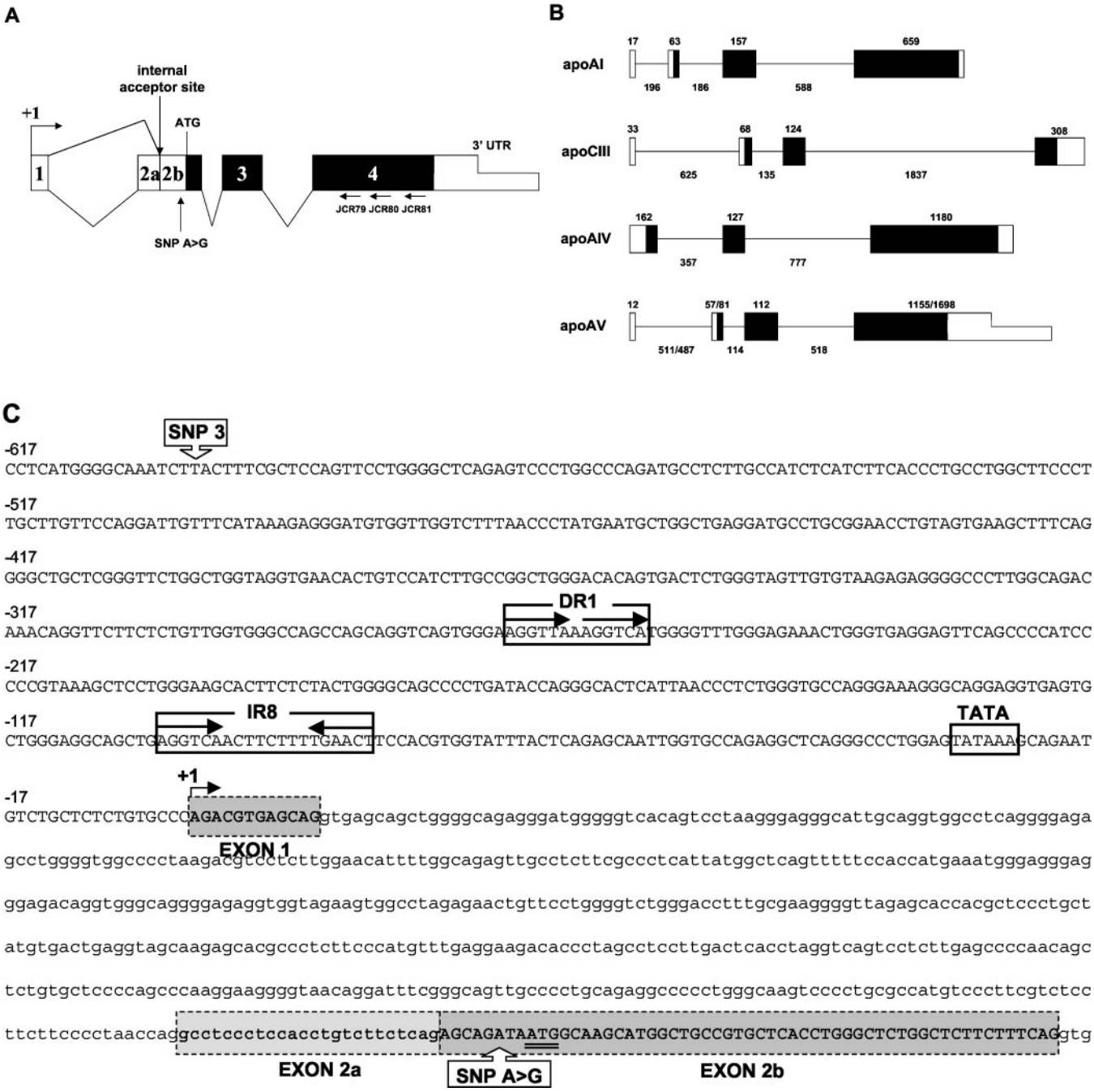

FIG. 1. **Characterization of the structure, the transcription start site, and the promoter of the human apoAV gene.** *A*, schematic representation of the exon-intron structure of the human apoAV gene. Exons are shown in *boxes* with translated regions *shaded* in *black*. The predicted initiation codon *ATG* is located in the second exon. The relative positions of the gene-specific primers used in the RLM-RACE are indicated by *horizontal arrows*. The last exon has two alternative polyadenylation sites (39), and the second exon has two alternative acceptor sites. A *bent arrow* depicts the transcription start site. The relative position of an SNP (A→G) is shown. *B*, the structure of the human apoAV gene is compared with that of the other components of the human apolipoprotein gene cluster. The structures of human apoAI and apoCIII genes are deduced from sequences in NM_000039, NM_000040, X01038, X03120, and J00098. The structure of the apoAIV gene is taken from Ref. 50. The exon lengths in nt are indicated by *numbers above* the *bars*. *Numbers below* the *lines* depict intron lengths. *C*, nucleotide sequence corresponding to the 5′ region of the human apoAV gene. Exons are in *boldface*. Intron sequences are shown in *lowercase*. The predicted initiation codon is *double underlined*. Numbers are relative to the transcription start site (+1). A putative TATA box and the DR1 and IR8 elements described in the current study are *boxed*. The consensus receptor-binding hexads are indicated by *horizontal arrows*.

metabolism. Pennacchio *et al.* (38) described the discovery of apoAV when 200 kb of orthologous sequences spanning the apoAI/CIII/AIV gene cluster were compared in humans and mice. At the same time, van der Vliet *et al.* (39) identified apoAV as a protein associated with an early phase of liver regeneration. Interestingly, the predicted amino acid sequence showed appreciable homology with apoAI and apoAIV. Evidence for the involvement of apoAV in triglyceride metabolism was obtained in mice, in which serum triglyceride concentrations were decreased to one-third when a human apoAV transgene was overexpressed (38) or adenoviral vectors expressing mouse apoAV were injected (40). Conversely, plasma triglyceride levels were 4-fold elevated in knockout mice lacking apoAV compared with their wild-type littermates (38). Furthermore, single nucleotide polymorphisms (SNPs) across the locus of the apoAV gene were found to be significantly associated with

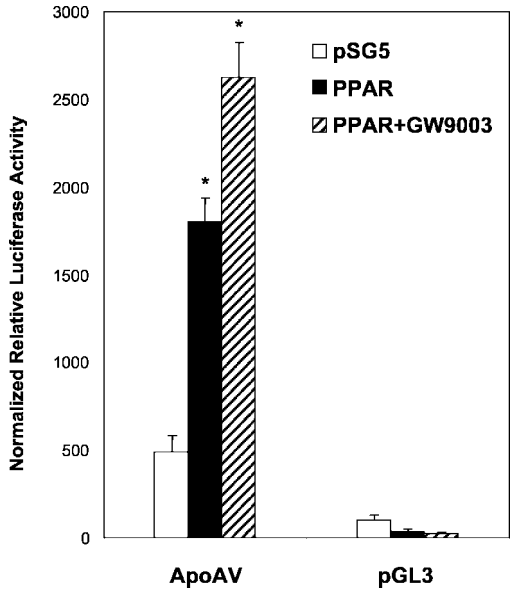

FIG. 2. **Transactivation of the human apoAV gene promoter by PPARα.** Hep3B cells were transfected with a plasmid containing a luciferase reporter gene driven by the 5′-flanking region (−617/+18) of the human apoAV gene or the empty pGL3-basic vector along with a plasmid expressing human PPARα or the empty vector pSG5 as control. Cells were treated with vehicle alone or 1 μM GW9003 for 48 h, and luciferase activities were measured and expressed as described under "Experimental Procedures." *, $p < 0.001$ *versus* control.

plasma triglyceride and very low density lipoprotein mass levels in several ethnic groups (38, 41–45). Notwithstanding, the specific biological functions of apoAV in triglyceride metabolism or liver regeneration are still unknown. Pennacchio *et al.* (38) reported a genomic organization of human apoAV with four exons. In contrast, van der Vliet *et al.* (39) reported three exons. Both groups showed that the expression of apoAV mRNA was restricted to the liver.

The current studies were undertaken to provide a comprehensive analysis of the regulation of human apoAV gene expression. We presently describe the genomic structure, the transcription start site, and the promoter of the human apoAV gene. Inasmuch as PPARα and FXR play key roles in the regulation of genes involved in triglyceride metabolism, we sought to evaluate their potential effects on human apoAV gene expression. We show that a novel FXRE is present in the promoter of human apoAV and demonstrate that human apoAV is a *bona fide* PPARα target gene. Our findings provide new insights into the mechanisms whereby PPARα and its ligands lower plasma triglyceride levels.

EXPERIMENTAL PROCEDURES

RNA Ligase-mediated Rapid Amplification of cDNA Ends (RLM-RACE)—The start of transcription of human apoAV was identified by using GeneRacer™ (Invitrogen). This kit provides a modification of the RACE method that ensures the capture of only full-length 5′ ends of specific transcripts via elimination of truncated messages from the amplification process. Human liver total RNA (Clontech) was treated with calf intestinal phosphatase and tobacco acid pyrophosphatase according to the instructions of the kit. After the selective ligation of an RNA oligonucleotide to the 5′-ends of decapped mRNA, first strand cDNA synthesis was carried out with the ThermoScript™ RNase H^- reverse transcriptase (Invitrogen; not supplied in the GeneRacer™ kit) at 50 °C for 50 min and a reverse human apoAV-specific primer (JCR81; see Table I). The cDNA 5′-end was amplified by using Platinum™ *Taq*DNA Polymerase High Fidelity (Invitrogen; not supplied in the GeneRacer™ kit) and primers GeneRacer™ 5′ and JCR80 (Table I). The PCR conditions were as follows: 94 °C for 2 min followed by 30 cycles of 94 °C for 30 s, 65 °C for 30 s, and 68 °C for 1 min. The sample was then diluted 20-fold, and 1 μl was used in a second PCR with nested primers (GeneRacer™ 5′ Nested and JCR79). DNA products were cloned into pCR4-TOPO™ vector (Invitrogen) and then sequenced.

Plasmids—Several constructs containing the 5′-flanking region of human apoAV (−2455/+18, −617/+18, −617/+529, −535/+18, −437/+18, −242/+18, and −82/+18, relative to the transcription start site reported in this paper) were obtained by PCR from human bacterial artificial chromosome-RPCI-11–442E11 DNA (BACPAC Resources, Children's Hospital Oakland Research Institute) with Platinum™ *Taq*DNA Polymerase High Fidelity (Invitrogen). Forward primers were tailed with a *Kpn*I restriction site. Reverse primers were tailed with an *Nhe*I site. The PCR products were digested with *Kpn*I and *Nhe*I and cloned into the corresponding sites of the promoterless firefly (*Photinus pyralis*) luciferase reporter plasmid pGL3-basic (Promega), generating p−2455/+18hAvLUC, p−617/+18hAvLUC, p−617/+529hAvLUC, p−535/+18hAvLUC, p−437/+18hAvLUC, p−242/+18hAvLUC, and p−82/+18hAvLUC. Site-directed mutagenesis of the constructs p−2455/+18hAvLUC, p−617/+18hAvLUC, and p−242/+18hAvLUC were accomplished using the QuikChange™ site-directed mutagenesis kit (Stratagene) according to the recommendations of the manufacturer. The vector pGL3-TK contains a fragment corresponding to nt −109 to +20 of the thymidine kinase (TK) gene promoter of herpes simplex virus (46) subcloned into the *Bgl*II/*Hin*dIII sites of the pGL3-basic vector. The reporter plasmids $p(AvIR8)_n$-TK (n = 1–4) were generated by insertion of 1–4 copies of a double-stranded oligonucleotide (obtained by annealing JCR139 and JCR140; see Table I) containing the sequences spanning nt −109 to −80 into the *Bgl*II site of pGL3-TK. Similarly, the four-copy mutant IR8 constructs $p(mt1AvIR8)_4$-TK, $p(mt2AvIR8)_4$-TK, and $p(mt3AvIR8)_4$-TK were generated by annealing oligonucleotides JCR159 with JCR160, JCR161 with JCR162, and JCR163 with JCR164, respectively, before ligation into *Bgl*II-digested pGL3-TK. The luciferase reporter plasmid $p(ER8)_4$-TK contains four copies of the rat MRP2 ER8 element (23) in front of TK promoter and was provided by L. Moore (GlaxoSmithKline, Research Triangle Park, NC). Plasmids expressing human cDNAs for PPARα, RXRα, and FXR were provided by J. A. Holt and J. M. Maglich (GlaxoSmithKline, Research Triangle Park, NC). The backbone of those plasmids was the mammalian expression vector pSG5 with a modified polylinker. Plasmid DNA was prepared using the Qiagen endotoxin-free maxipreparation method and quantitated spectrophotometrically. The integrities of all plasmids were verified by DNA sequencing.

Cell Transfection and Reporter Assays—Human hepatoblastoma Hep3B and monkey kidney CV-1 cell lines were cultured in Eagle's basal medium supplemented with nonessential amino acids, 2 mM L-glutamine, 100 units/ml penicillin, and 100 μg/ml streptomycin sulfate (medium A) and 10% (v/v) fetal calf serum (FCS). On day 0, cells were seeded on 24-well plates at a density of 3×10^5 or 5×10^4 cells/well for Hep3B or CV-1, respectively. On day 1, cells were transfected with FuGENE 6 reagent (Roche Applied Science) according to the manufacturer's instructions. Typically, each well of a 24-well plate received 100 ng of firefly luciferase reporter plasmid and, when indicated, 200 ng of plasmids expressing human PPARα or FXR. Effector plasmid dosage was kept constant by the addition of appropriate amounts of the empty expression vector pSG5. 100 ng/well of a sea pansy (*Renilla reniformis*) luciferase plasmid pRL-TK (Promega) was included in all transfections as an internal control for transfection efficiency. After 5 h, cells were switched to medium A supplemented with 10% delipidated calf serum (Sigma) in the presence, when indicated, of either 1 μM GW9003 (GlaxoSmithKline), 50 or 100 μM CDCA, 1 μM GW4064 (GlaxoSmithKline), or the vehicle (Me_2SO). On day 3, cell lysates were prepared by shaking the cells in 200 μl of 1× Promega lysis buffer for 15 min at room temperature. Firefly and *Renilla* luciferase activities were measured using a Dual-Luciferase® Reporter Assay System (Promega) and a Lumistar luminometer (BMG Lab Technologies). Firefly luciferase activity values were divided by *Renilla* luciferase activity values to obtain normalized luciferase activities. To facilitate comparisons within a given experiment, activity data were presented either as relative luciferase activities or as -fold induction over the normalized activity of the reporter plasmid in the absence of nuclear receptor cotransfection and agonist supplementation. All transfection experiments were performed at least three times and with each experimental point done in triplicate. The data are expressed as the means ± S.D. Statistic significance analysis were done with Student's t test.

Treatment of HepG2 Cells—On day 0, human hepatoblastoma HepG2 cells were plated on 24-well plates at 3.5×10^5 cells/well in medium A supplemented with 10% (v/v) FCS. On day 1, the medium was replaced with fresh medium A supplemented with 1% (v/v) FCS and 1 μM GW9003, 1 μM GW4064, or vehicle (Me_2SO). On day 3, the

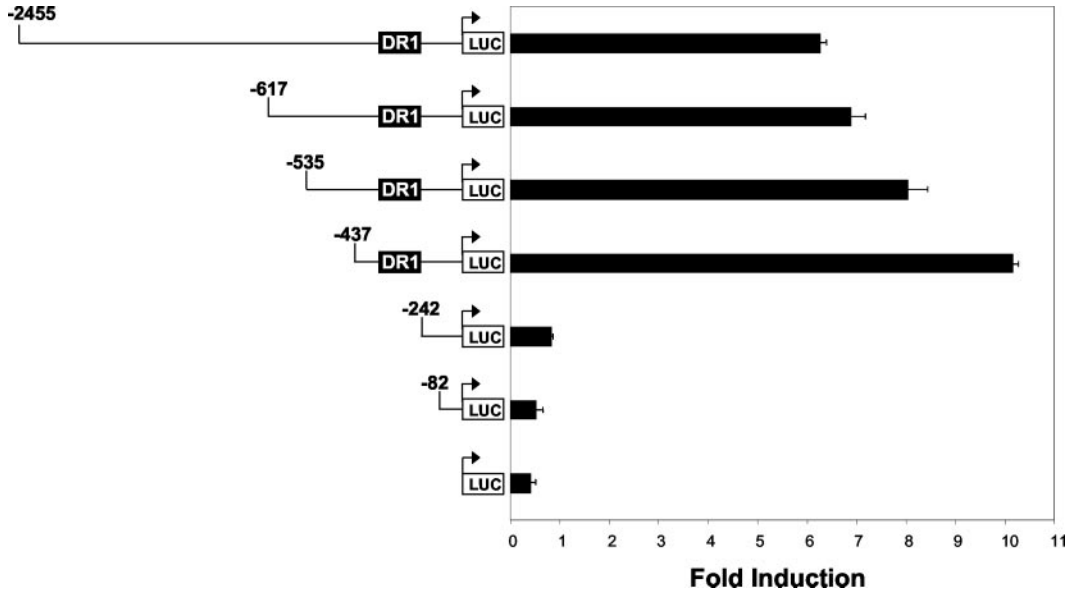

FIG. 3. **Localization of a PPARα response region in the human apoAV promoter by progressive deletion analysis.** Hep3B cells were cotransfected with reporter plasmids containing the firefly luciferase gene driven by progressively 5′-shortened fragments of the apoAV promoter as indicated together with the empty vector pSG5 or a plasmid expressing human PPARα. Cells were treated with vehicle or 1 μM GW9003 for 48 h, and luciferase activities were measured as described under "Experimental Procedures." Results are expressed as -fold induction over control. *LUC*, luciferase.

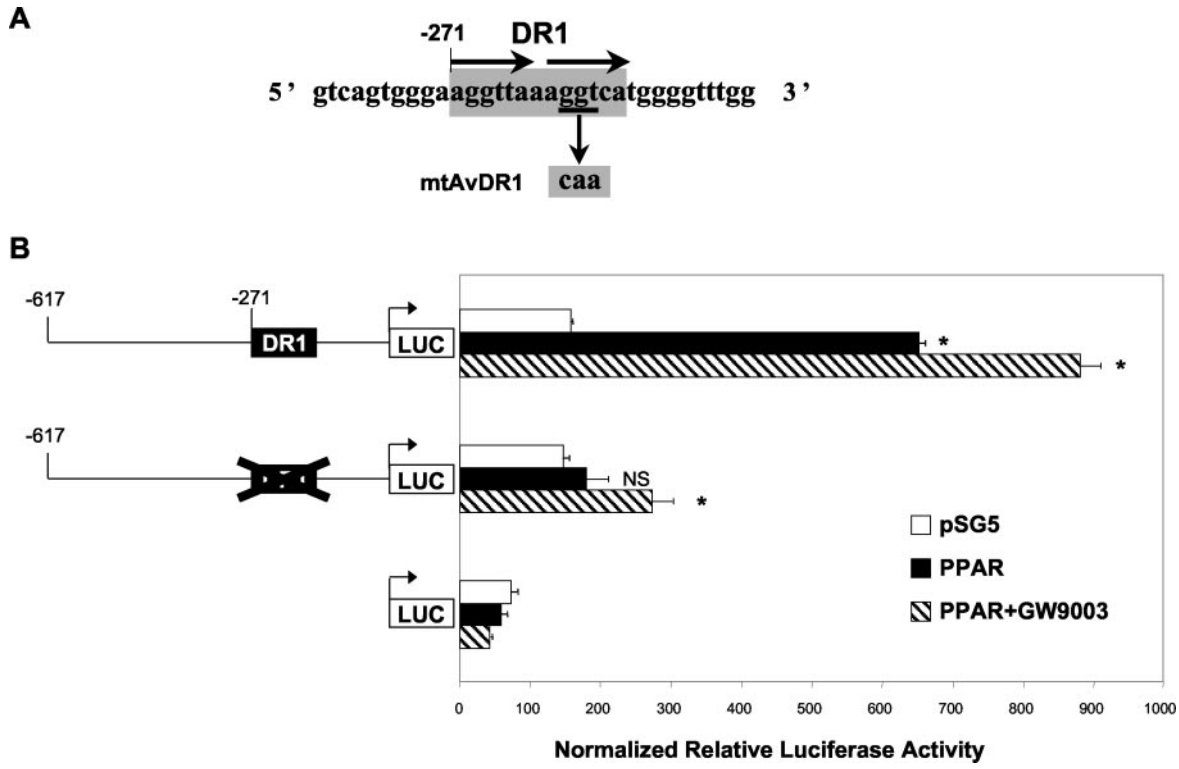

FIG. 4. **Functional effects of mutations in the DR1 element on the response of the human apoAV promoter to PPARα.** *A*, human apoAV gene promoter sequence surrounding the DR1 element. The *gray box* denotes the DR1 sequence. The AGGTCA half-sites are indicated by *horizontal arrows*. The wild-type nucleotides that were modified by site-directed mutagenesis are *underlined*. The corresponding −263G→C/−262G→A/−261T→A mutated nucleotides are shown *below* the *vertical arrow* and *within* the *gray square*. *B*, Hep3B cells were transfected with a plasmid expressing human PPARα or the empty pSG5 vector as control together with reporter constructs containing the wild-type or site-directed mutated 5′-flanking regions (−617/+18) of the human apoAV gene or the empty pGL3-basic vector as negative control. Cells were treated with vehicle or GW9003 (1 μM) for 48 h, and luciferase activities were measured and expressed as described under "Experimental Procedures." *, $p < 0.05$ *versus* control. *NS*, not significant. The *cross* depicts the presence of site-directed mutations in the DR1 element. *LUC*, luciferase.

cells were washed twice with phosphate-buffered saline and harvested for isolation of RNA.

Treatment of Primary Cultured Cynomolgus Monkey Hepatocytes—Cynomolgus monkey hepatocytes (batch L-1811; Biopredict) were seeded on day 0 at a density of 6×10^5 cells/well on 12-well plates in Williams' medium E supplemented with 2 mM L-glutamine, 100 units/ml penicillin, 100 μg/ml streptomycin sulfate, 4 μg/ml insulin (medium B), and 10% (v/v) FCS. On day 1, cells were switched to medium B containing 100 nM dexamethasone, 1% (v/v) FCS and 1 μM GW9003, 1 μM GW4064, 30 μM lithocholic acid (LCA), or vehicle (Me_2SO). After 24 h, a fresh experimental medium was provided. On day 3, the cells were washed twice with PBS and harvested for isolation of RNA.

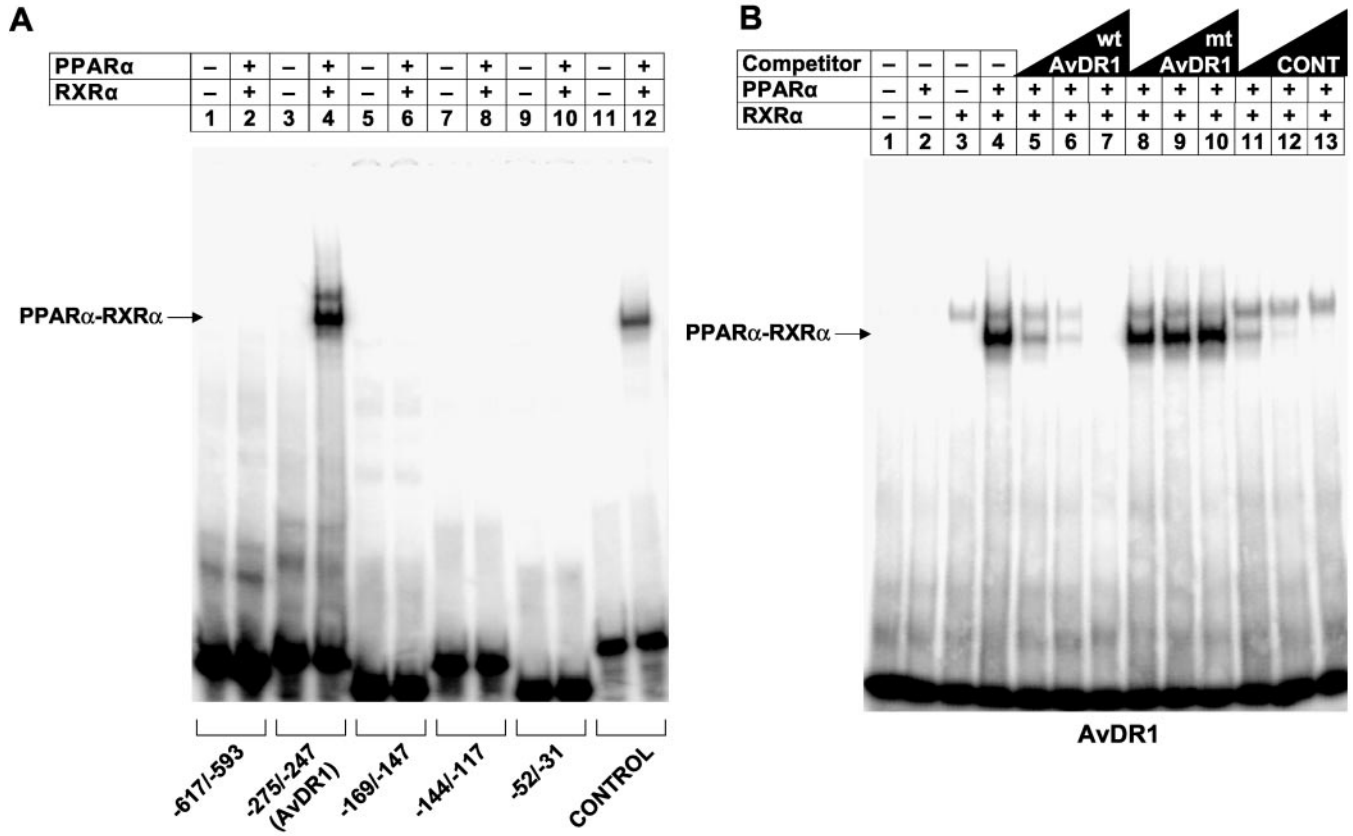

FIG. 5. **PPARα-RXRα heterodimers can specifically bind to the DR1 element of the human apoAV promoter.** *A*, EMSAs were performed using *in vitro* transcribed/translated human PPARα (2.5 μl), human RXRα (2.5 μl), or unprogrammed reticulocyte lysate (−), when indicated, and labeled double-stranded oligonucleotides corresponding to the indicated fragments of the human apoAV gene promoter as described under "Experimental Procedures." The lysate volumes were kept constant by the addition of unprogrammed lysate. *CONTROL*, a labeled probe that contains the PPRE of the mitHMGS gene (3-fold less was used). *B*, competition experiments for binding of PPARα-RXRα heterodimers to the labeled double-stranded oligonucleotides corresponding to nt −275 to −247 (*AvDR1*) were performed by adding a 10-, 50-, and 250-fold molar excess of the indicated unlabeled probes. *mtAvDR1* is a modified version of *wtAvDR1* with mutations corresponding to nt −263G→C/−262G→A/−261T→A. The specific PPARα-RXRα-PPRE complex is indicated by an *arrow*. *CONT*, PPRE of mitHMGS gene (48); *wt*, wild type; *mt*, mutated.

Real Time PCR Quantification of mRNAs—Total RNA was prepared from primary cynomolgus hepatocytes, human THP-1 monocytes differentiated to macrophages, HepG2, Hep3B, Huh-7, and Caco-2 cells with the RNeasy™ Mini kit, the QIAshredder™ homogenizers, and the RNase-Free DNase set (Qiagen) according to the manufacturer's instructions. A 1-μg aliquot was used as a template for cDNA synthesis, employing the TaqMan™ Reverse Transcription Reagents kit (Applied Biosystems). Specific primers for each gene were designed with Primer Express Software (PerkinElmer Life Sciences). The sequences of forward and reverse primers are shown in Table I. The specificity of the primers was verified by showing that the real time reverse transcriptase (RT)-PCR reaction product generated a single band after agarose gel electrophoresis. In addition, each couple of primers was tested in successive dilutions of cDNA to analyze and validate its efficiency. The reactions contained, in a final volume of 25 μl, 5 μl of diluted (1:10) cDNA, a 300 nM concentration of the forward and reverse primers, and 2× SYBR™ Green PCR Master Mix (Applied Biosystems). Real time PCRs were carried out in 96-well plates by using the ABI PRISM™ 7700 sequence detection system (Applied Biosystems). Since there is a high level of sequence identity for apoAV between humans and monkeys, the primers were valid for RNA from both primates. Levels of apoAV were normalized to 18 S to compensate for variations in input RNA amounts (18 S levels were unaffected by the treatments). All points were performed in triplicate during two independent experiments, and the RT-PCRs were carried out in duplicate for each sample. The relative amounts of mRNAs were calculated using the Comparative C_T method as described in Ref. 55.

In Vitro Transcription/Translation and Electrophoretic Mobility Shift Assay (EMSA)—Human PPARα, RXRα, and FXR proteins were synthesized *in vitro* from the corresponding expression plasmids in rabbit reticulocyte lysate by using the TNT® Quick Coupled transcription/translation system (Promega) according to the instructions of the manufacturer. In order to obtain an unprogrammed lysate as a negative control for EMSA, a reaction was performed with the empty vector pSG5. Double-stranded oligonucleotides were radiolabeled by fill in with the Klenow fragment of DNA polymerase I and used as probes. For competition experiments, increasing -fold molar excesses of unlabeled probes were included during a 15-min preincubation on ice. Protein-DNA binding assays were performed as described (47). AvDR1 is a double-stranded oligonucleotide corresponding to nt −275 to −247 of human apoAV promoter. mtAvDR1 is a modified version of AvDR1 that contains mutations corresponding to nt −263(G→C)/−262(G→A)/−261(T→A). The control probe used in EMSA with PPARα-RXRα contains the PPRE of the rat mitochondrial 3-hydroxy-3-methylglutaryl-CoA synthase (mitHMGS) gene promoter (48). The probe AvIR8 contains the sequence spanning nt −109 to −80 of the human apoAV promoter. The mutations present in the modified versions of AvIR8 (mt1AvIR8, mt2AvIR8, and mt3AvIR8) are shown in Fig. 10*B*. The probe used as a control for competition experiments with FXR-RXRα contains the FXRE of the human I-BABP gene promoter (30). Samples were electrophoresed at 4 °C on a 4.5% polyacrylamide gel in 0.5× TBE buffer (45 mM Tris, 45 mM boric acid, 1 mM EDTA, pH 8.0). Gels were dried and analyzed using an Amersham Biosciences PhosphorImager STORM 860 and ImageQuant software (Amersham Biosciences).

RESULTS

Characterization of the Structure of the Human ApoAV Gene, Identification of an Alternatively 5′-Untranslated Region, and Determination of the Transcription Start Site—Two previous reports coincided to show by Northern blot analysis that apoAV has transcripts of ~1.3 and 1.9 kb in the human liver, which are likely to result from alternative polyadenylation (38, 39). However, the number of exons and the details of the exon/intron organization in the 5′ region of the human apoAV gene

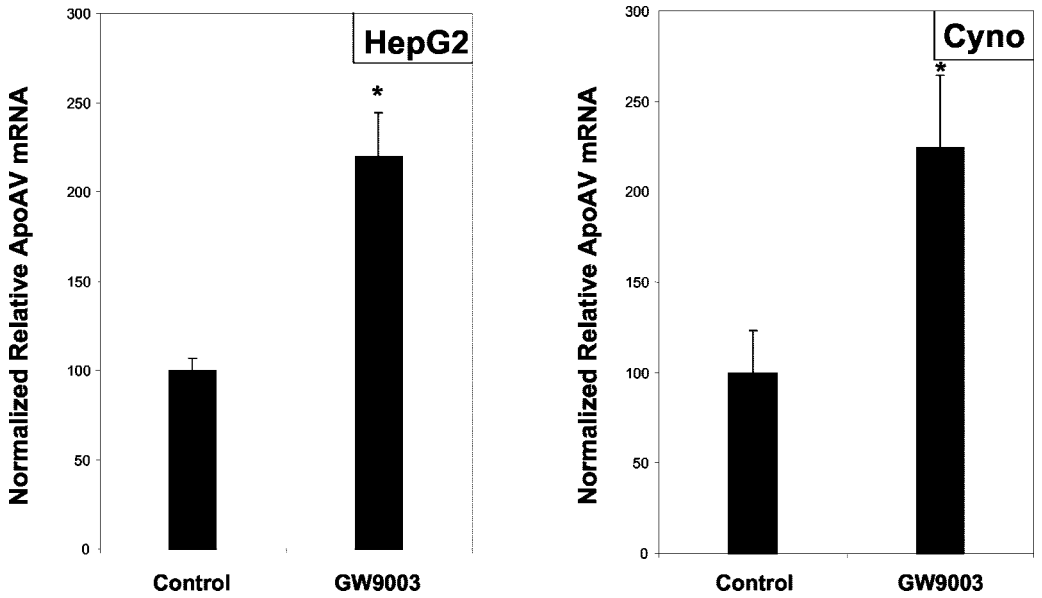

FIG. 6. **PPARα agonists enhance apoAV mRNA levels in human HepG2 cells and primary cynomolgus hepatocytes.** Hepatocytes isolated from cynomolgus liver (*Cyno*) and human hepatoma HepG2 cells were treated for 48h with vehicle (*Control*) or 1 μM GW9003. Total RNA was extracted for analysis by real time RT-PCR as described under "Experimental Procedures." Specific apoAV mRNA levels normalized to 18 S content are expressed relative to untreated cells set as 100 (mean ± S.D.). *, $p < 0.01$ *versus* control.

have been contradictory. In order to delineate the structure of the gene, we performed RLM-RACE. This powerful technique is a modification of the RACE method that ensures the capture of only full-length specific transcripts via elimination of truncated messages from the amplification process. Thus, using antisense primers from the 3′ region of mRNA, it is possible to amplify all of the upstream exons and hence to detect the presence of alternatively spliced exons. A primer was designed at the last exon of human apoAV, and a specific reverse transcription was carried out from human liver RNA. In order to avoid secondary structures of mRNA, we made the first strand cDNA synthesis at 50 °C with a reverse transcriptase having a high thermal stability (see "Experimental Procedures"). Subsequently, specific PCRs were performed using additional apoAV nested primers (Table I). The PCR products were cloned and sequenced. Based on the genomic sequence spanning part of human chromosome 11q23 present in the GenBank™ data bank (accession number AC007707), we obtained an exon/intron organization of apoAV with two distinct 5′-untranslated regions (Fig. 1*A*). As shown in Fig. 1*B*, the four-exon structure of apoAV is also present in apoAI and apoCIII genes (as deduced from the analysis of sequences in NM_000039, NM_000040, X01038, X03120, and J00098) but not in apoAIV (structure taken from Ref. 50). The most important feature of the RLM-RACE method is that it permits the determination of the transcription start site with more precision than the primer extension and the classic 5′-RACE procedures. As shown in Fig. 1*C*, a single human apoAV transcription start site was identified. The newly identified first exon, which was named exon 1, has only 12 untranslated nt and contains a stop codon in frame with the first ATG, which is located in the following exon (Fig. 1*C*). Interestingly, a sequence of 24 nt was observed just after exon 1 in 4 of 20 clones. This novel sequence, which we named exon 2a, was flanked on the 5′ side by an ag consensus splice acceptor site on the first intron and on the 3′ side by the exon previously described in the literature as exon 1, which we renamed exon 2b (Fig. 1*C*). Therefore, the second exon has either 57 nt (exon 2b) or 81 nt (exon 2a plus exon 2b), depending on the utilization of an internal acceptor site (Fig. 1*A*). No novel exons were observed, so the coding region is distributed in three exons, in agreement with earlier results (39). Considered together, the human apoAV gene consists of four exons, the second exon with two alternative acceptor sites and the last exon with two alternative polyadenylation sites. On the other hand, we noticed the presence of an SNP (A→G) 3 nt upstream from the predicted translation start codon (Fig. 1*C*).

Expression of ApoAV in Human Cell Lines—Previously published Northern blots with RNA from several different human tissues have shown that apoAV expression is restricted to the liver (38, 39). We carried out real time PCR quantification assays with RNA from several human cell lines with different origins. We found that apoAV is expressed in HepG2 and Hep3B hepatoma cells with levels comparable with the liver, but not in hepatic Huh-7 cells. Consistent with the hepatic specific expression, intestinal Caco-2 cells and THP-1 monocytes differentiated to macrophages showed no detectable expression of apoAV (data not shown).

Cloning and Characterization of the Human ApoAV Gene Promoter—Analysis of the 5′-flanking region of the human apoAV gene identified a TATA box 30 nt upstream of position +1 (Fig. 1*C*), further confirming the mapped transcription start site. No consensus Sp1 binding sites were found within the first 3 kb, although several putative nuclear receptor response elements containing imperfect repeats of the half-site PuGGTCA were detected (see below). To investigate whether this 5′-flanking region could drive transcription of a reporter gene, we subcloned ~0.6 kb of the human apoAV sequence upstream of the transcription start site into the firefly luciferase pGL3-basic vector. The resulting construct, p−617/+18hAvLUC, was transiently transfected into HepG2 and Hep3B cells. The activity of this construct was about 5-fold the activity of the parental promoterless vector in both cell lines (Fig. 2). Next, we observed that neither the addition of a more upstream region, in construct p−2455/+18hAvLUC, nor the inclusion of the first intron, in p−617/+529hAvLUC, substantially altered promoter activity (data not shown).

Overexpression of the Nuclear Receptor PPARα Enhances the Activity of the Human ApoAV Gene Promoter—ApoAV is an important determinant of plasma triglyceride levels (38, 40–45). Inasmuch as PPARα regulates the expression of genes involved in triglyceride metabolism (10), we evaluated whether this nu-

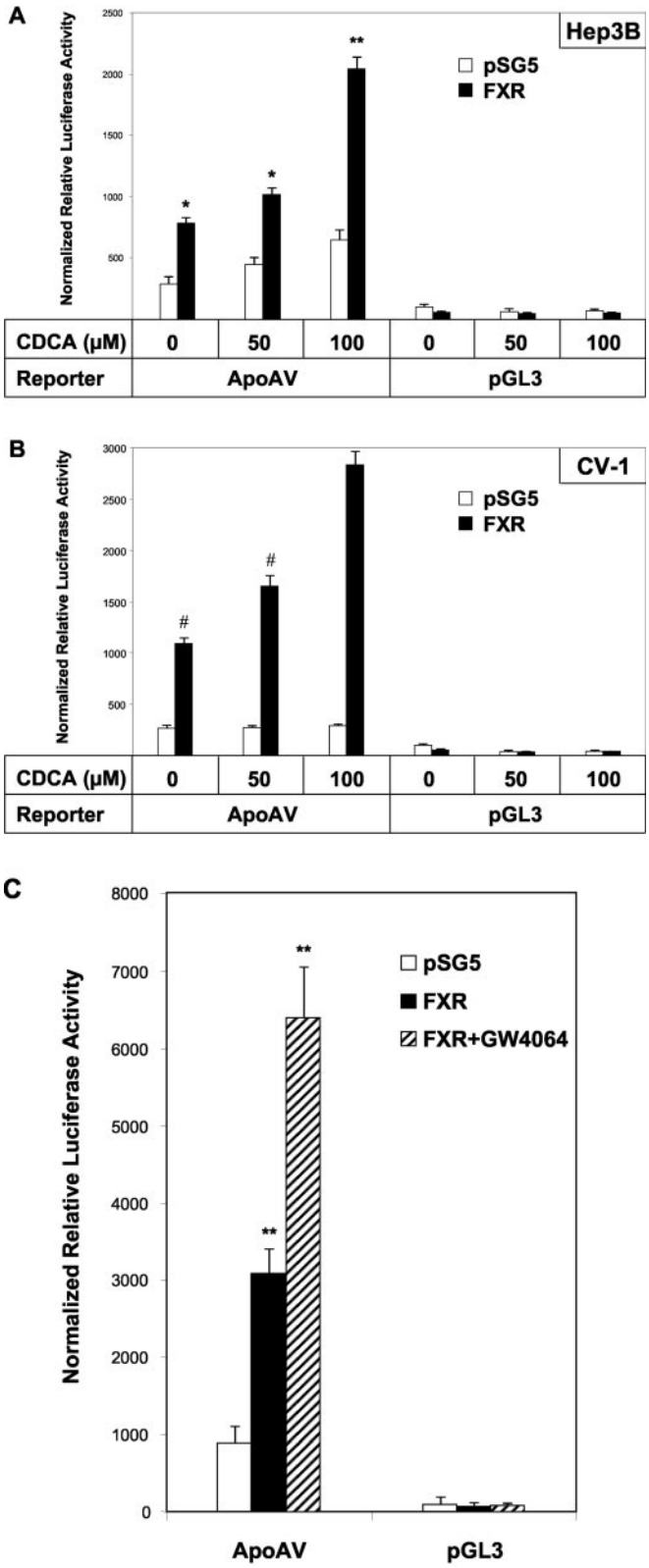

FIG. 7. **Bile acids induce human apoAV promoter activity via FXR.** Hep3B (*A* and *C*) and CV-1 (*B*) cells were transfected with a plasmid containing a luciferase reporter gene driven by the 5′-flanking region (−617/+18) of the human apoAV gene or the empty pGL3-basic vector along with a plasmid expressing human FXR or the empty vector pSG5 as control. Cells were treated for 48 h with vehicle alone, with increasing concentrations of CDCA (*A* and *B*), or with 1 μM GW4064 (*C*), and luciferase activities were measured and expressed as described under "Experimental Procedures." Significant differences compared with the corresponding pSG5 control are as follows: *, $p < 0.005$; **, $p < 0.001$; #, $p < 0.0005$.

clear receptor modulates human apoAV gene expression. For this purpose, transient transfection studies were performed in Hep3B cells. Cotransfection of a human PPARα expression plasmid resulted in a significant increase of the activity of the firefly luciferase reporter gene driven by the −617/+18 sequence of the human apoAV promoter (Fig. 2). The effect of PPARα overexpression was promoter-dependent, because it was not observed with the promoterless pGL3-basic vector. In line with previous studies in hepatic cells (48, 49), transiently transfected PPARα showed substantial constitutive activity, possibly due to activation by endogenous ligands. Nevertheless, we observed that it could be further activated upon the exogenous addition of the specific PPARα ligand GW9003 (Fig. 2).

Mapping of the Human ApoAV Promoter Site Conferring Responsiveness to PPARα—In order to localize the region required for PPARα activation, a series of progressively larger 5′-deletion human apoAV promoter constructs from nt −2455 to +18 were transiently transfected into Hep3B cells together with a human PPARα expression plasmid in the presence or absence of GW9003. As shown in Fig. 3, the sequence upstream to position −437 can be deleted without loss of the response to PPARα. However, further deletion up to nt −242 eliminated the PPARα responsiveness. Analysis of the sequence in the −437/−242 fragment revealed two potential hexamer binding sites separated by a single nucleotide between nt −271 and −259 (Fig. 1*C*), thereby conforming to the DR1 response element for PPARα (PPRE).

To unequivocally characterize the DR1 as a PPRE, Hep3B cells were cotransfected with a human PPARα expression vector and an apoAV promoter-luciferase reporter plasmid in which the DR1 sequence was mutated in the 3′-hexamer (Fig. 4*A*). In contrast to the native promoter construct, PPARα and GW9003 had only a modest residual effect on the luciferase gene expression of the construct bearing the mutated DR1 (Fig. 4*B*). These results demonstrate that this DR1 indeed confers PPARα response to the apoAV promoter.

Binding Analysis of PPARα-RXRα Heterodimers to the apoAV DR1 Element—PPARα binds to DNA as a heterodimer with RXR (10). To investigate whether PPARα-RXR heterodimers directly bind to the human apoAV gene promoter, radiolabeled double-stranded oligonucleotides corresponding to portions of the −617/+18 fragment of the apoAV promoter were used as probes in EMSA experiments (Fig. 5). As expected, the addition of *in vitro* translated PPARα and RXRα proteins resulted in the appearance of a robust retarded complex when using a −275/−247 fragment containing the apoAV DR1 (Fig. 5*A*, *lane 4*), but not when −617/−593, −169/−147, −144/−117, and −52/−31 probes (Fig. 5*A*, *lanes 2*, *6*, *8*, and *10*, respectively) or −484/−462, −399/−374, −298/−263, and −109/−80 fragments were employed (data not shown). Furthermore, the specificity of the RXRα-PPARα heterodimer-apoAV DR1 interaction was demonstrated by competition analysis. The formation of the retarded complex was inhibited by the addition of increasing concentrations of either the unlabeled apoAV DR1 probe (Fig. 5*B*, *lanes 5–7*) or a cold probe containing the PPRE of the mitHMGS gene (Fig. 5*B*, *lanes 11–13*). In contrast, a cold double-stranded oligonucleotide that is equivalent to the apoAV DR1 probe but harbors point mutations in the 3′ half-site (nt −263G→C/−262G→A/−261T→A in Fig. 4*A*) could not displace the labeled wild-type element (Fig. 5*B*, *lanes 8–10*). In addition, it is worth noting that a more retarded band of the labeled apoAV DR1 containing probe was visible upon the addition of RXRα alone (Fig. 5*B*). Further investigations will be done to elucidate the nature of this band. Taken together, these results show that this apoAV DR1 is a genuine PPRE.

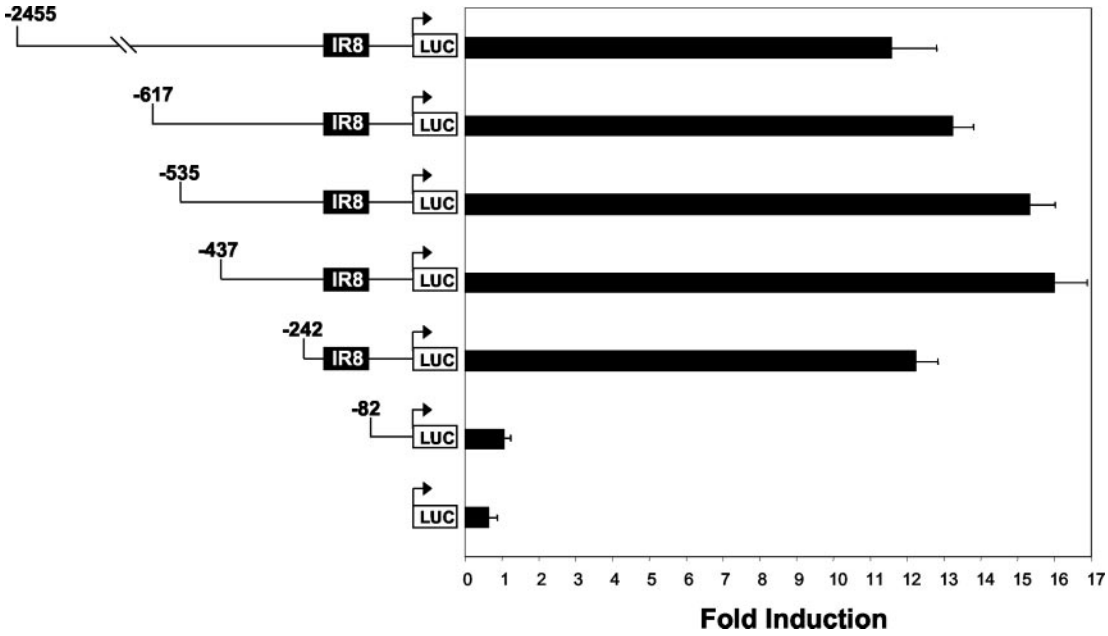

FIG. 8. **The region between nt −242 and −82 of the human apoAV promoter mediates the response to bile acid-activated FXR.** CV-1 cells were cotransfected with reporter plasmids containing the firefly luciferase gene driven by progressively 5′-shortened fragments of the apoAV promoter together with the empty vector pSG5 or a plasmid expressing human FXR. Cells were treated with vehicle or 100 μM CDCA for 48 h, and luciferase activities were measured as described under "Experimental Procedures." Results are expressed as -fold induction over control. *LUC*, luciferase.

PPARα Agonists Induce ApoAV mRNA Levels in Human Hepatoma HepG2 Cells and Primary Cultures of Cynomolgus Hepatocytes—To analyze whether apoAV mRNA expression is regulated by PPARα agonists, primary hepatocytes isolated from cynomolgus liver and human hepatoma HepG2 cells were incubated for 48 h in medium containing GW9003 or vehicle. As determined by quantitative real time RT-PCR, treatment with the PPARα agonist markedly increased apoAV mRNA levels (Fig. 6).

Bile Acids Induce Human apoAV Gene Promoter Activity via the Nuclear Receptor FXR—FXR regulates lipoprotein metabolism (16), and FXR agonists have hypotriglyceridemic effects on rodents and humans (34, 35, 37). To determine whether FXR and bile acids are able to modulate the apoAV gene promoter activity, transient transfection assays were performed with a firefly luciferase reporter gene expression vector driven by the −617/+18 sequence of the human apoAV promoter. In Hep3B, the bile acid CDCA alone induced apoAV promoter activity to some extent (Fig. 7*A*). Cotransfection of a human FXR expression plasmid significantly enhanced CDCA-induced promoter activity. To further confirm the role of FXR in the bile acid-induction of the apoAV promoter, monkey kidney CV-1 cells, a cellular model frequently used in order to avoid the background of endogenous FXR (19–21, 32), were also employed. As shown in Fig. 7*B*, promoter activity was unaffected by CDCA in the absence of FXR supplied exogenously. By contrast, cotransfection of FXR led to a more than 10-fold induction of apoAV promoter activity in the presence of 100 μM CDCA. In both cell lines, the transactivation of the apoAV promoter-luciferase reporter plasmid by CDCA via FXR was dose-dependent (Fig. 7, *A* and *B*). Moreover, the effects of CDCA and FXR were promoter-dependent, because they were not observed with the promoterless pGL3-basic vector. Since bile acids may also exert their actions through FXR-independent pathways, we also tested the synthetic nonsteroidal specific FXR ligand GW4064 (34). As expected, treatment of Hep3B cells with GW4064 further enhanced the transactivation of the apoAV promoter by FXR (Fig. 7*C*). These data clearly demonstrated the existence of an FXR response element in the promoter of the human apoAV gene.

A Novel Element in the Human ApoAV Promoter Is Required for Transcriptional Activation by FXR—To localize the region within the human apoAV promoter that confers transcriptional responsiveness to FXR and bile acids, a series of constructs containing sequential 5′-deletions from nt −2455 to +18 of the apoAV promoter in front of the firefly luciferase reporter gene were transiently transfected into CV-1 cells together with a human FXR expression plasmid in the presence or the absence of 100 μM CDCA (Fig. 8). The results showed that the nucleotide sequence between −2455 and −242 could be removed without preventing strong activation of the reporter gene by bile acid-activated FXR. In contrast, deletion of the fragment between nt −242 and −82 completely abolished the induction of apoAV promoter activity by CDCA-activated FXR, indicating that this region mediates the effects of bile acids.

Surprisingly, analysis of the sequence in the −242/−82 fragment did not reveal any of the previously described FXR response element (IR0, IR1, or ER8) motifs (16, 22, 23). The only repeat of the hexanucleotide core motif PuGGTCA with a low degree of degeneration present within this region corresponds to an inverted repeat separated by 8 nucleotides (IR8) between nt −103 and −84 (Fig. 1*C*). Although a response element with this kind of organization has never been reported before, we mutated both halves of the IR8 site (Fig. 9*A*) in the context of the apoAV promoter on both the longest plasmid (Fig. 9*B*) and the shortest construct that still responds to FXR (Fig. 9*C*) and performed transient transfections in Hep3B cells. Whereas cotransfection of an FXR expression plasmid significantly enhanced wild-type apoAV promoter activity, FXR failed to induce the activity of the mutated constructs. These results unequivocally show that this IR8 element is required for the response to FXR and that there is no other FXRE in the promoter of human apoAV.

The ApoAV IR8 Element Confers FXR Responsiveness to Heterologous Promoters—To evaluate whether this IR8 element could confer FXR responsiveness to a heterologous promoter, we linked the apoAV IR8 site upstream of the TK promoter and the luciferase reporter gene. Reporter constructs containing

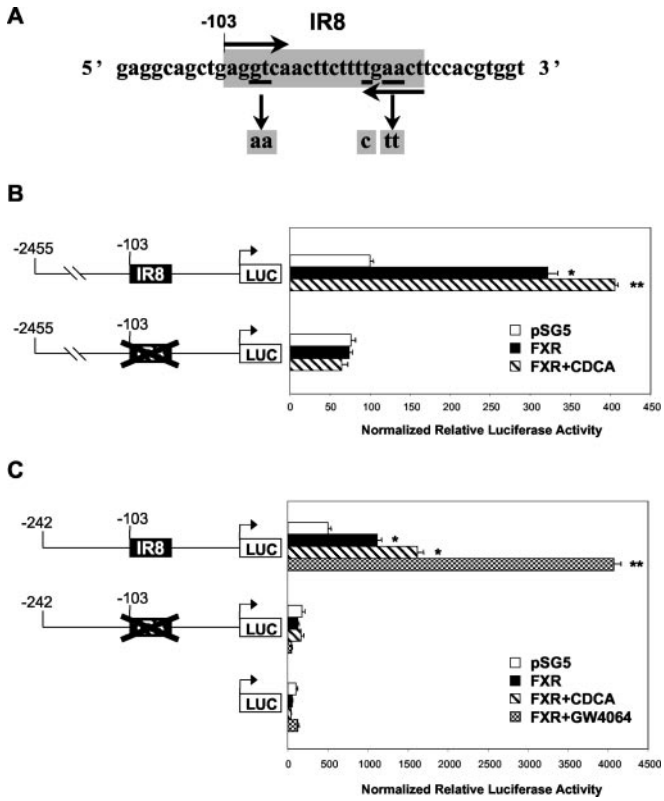

FIG. 9. **Mutation of the IR8 element on the human apoAV promoter eliminates the response to FXR.** *A*, human apoAV gene promoter sequence surrounding the IR8 element. The *gray box* denotes the IR8 sequence. The AGGTCA half-sites are indicated by *horizontal arrows*. The wild-type nucleotides that were modified by site-directed mutagenesis are *underlined*. The corresponding mutated nucleotides are shown *below* the *vertical arrows* and within the *gray squares*. *B* and *C*, Hep3B cells were transfected with a plasmid expressing human FXR or the empty pSG5 vector as control together with reporter constructs containing the wild-type or site-directed mutated 5′-flanking regions of the human apoAV gene or the empty pGL3-basic vector as negative control. Cells were treated for 48 h with vehicle, 100 μM CDCA, or 1 μM GW4064, and luciferase activities were measured and expressed as described under "Experimental Procedures." Significant differences compared with the corresponding pSG5 control are as follows: *, $p < 0.001$; **, $p < 0.0005$. The *crosses* depict the presence of site-directed mutations in the IR8 element. *LUC*, luciferase.

1–4 copies of the apoAV IR8 element were transiently transfected into Hep3B cells along with a human FXR expression plasmid in the presence or the absence of CDCA. As demonstrated in Fig. 10*A*, bile acid-activated FXR enhanced the activity of apoAV IR8-driven promoter constructs, whereas the reporter construct with the TK promoter alone was not stimulated at all. Indeed, an induction of about 50-fold was reached with four copies, and the response was manifested in a copy number-dependent manner, thereby confirming that the IR8 element functions as an FXRE.

Next, the effects of selective mutations of each half-site in the IR8 element (Fig. 10*B*) were examined in Hep3B cells transfected with reporter constructs driven by four copies of the apoAV IR8 in front of the TK promoter. The FXR-dependent induction was abrogated when mutations were introduced in any half-site (Fig. 10*C*). These observations confirm the organization of this FXR response element as an inverted repeat of the canonical hexanucleotide separated by 8 nt. Finally, the ability of the apoAV IR8 to respond to FXR and bile acids was assessed by comparison with the ER8 element described in the promoter of MRP2 gene (23). The FXR-dependent response of the MRP2 ER8 in front of TK was ~2.5-fold higher than the apoAV IR8 (Fig. 10*A*).

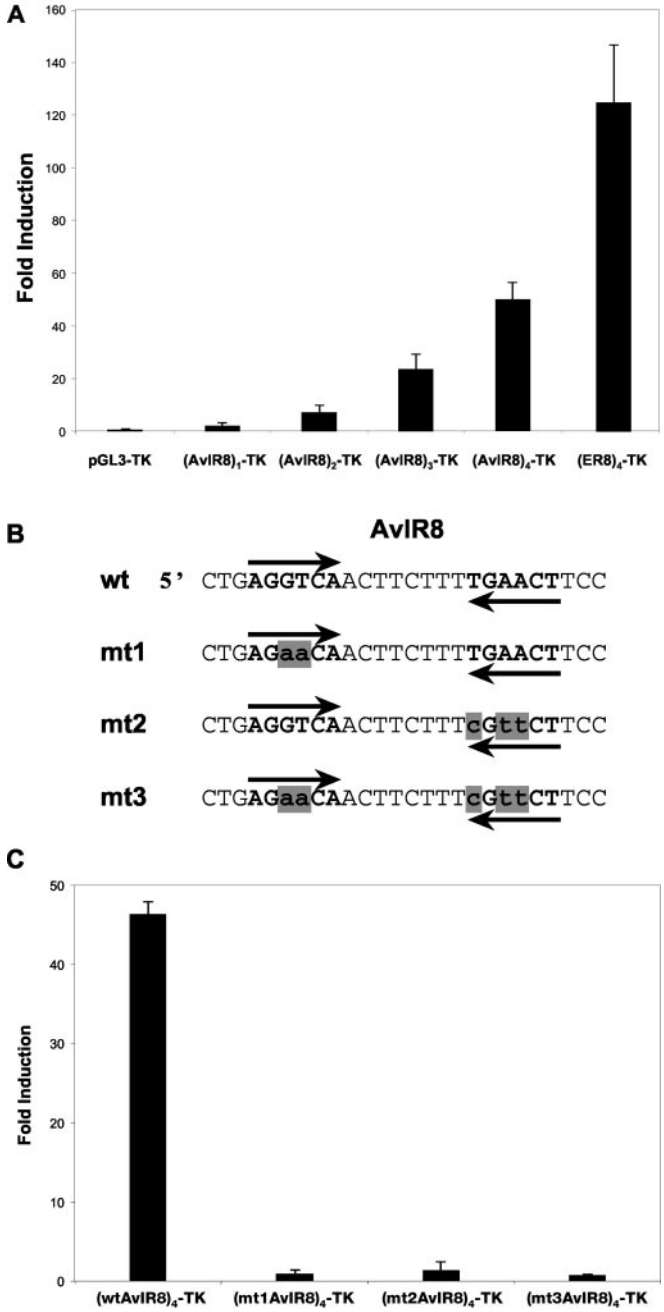

FIG. 10. **The IR8 element present in the promoter of the human apoAV gene (AvIR8) confers FXR responsiveness to heterologous promoters.** *A*, the apoAV IR8 element confers transactivation by bile acid-activated FXR in a copy number-dependent manner. Hep3B cells were transiently transfected with plasmids expressing human FXR or the empty pSG5 vector as control, together with reporter constructs containing 1–4 copies of the sequence corresponding to nt −109 to −80 (*AvIR8*) of the human apoAV gene promoter or four copies of the ER8 element present in the MRP2 gene promoter (*ER8*) cloned in front of a heterologous TK promoter-driven luciferase. The empty pGL3-TK reporter vector was used as negative control. Cells were treated with vehicle or 100 μM CDCA for 48 h, and luciferase activities were measured as described under "Experimental Procedures." Results are expressed as -fold induction over control. *B*, human apoAV gene promoter sequence surrounding the IR8 element and mutated versions used in *C*. The hexameric consensus sites are in *boldface type*, and their orientations are indicated by *arrows*. Mutations in half-sites are shown in *lowercase type* and within *gray squares*. *C*, functional effects of mutations on hexameric consensus sites. Experiments were performed as in *A* with reporter constructs containing four copies of the wild-type (*wt*) (*wtAvIR8*) or mutant (*mt1AvIR8*, *mt2AvIR8*, *mt3AvIR8*) sequences corresponding to nt −109 to −80 of the human apoAV gene promoter cloned in front of TK promoter-driven luciferase.

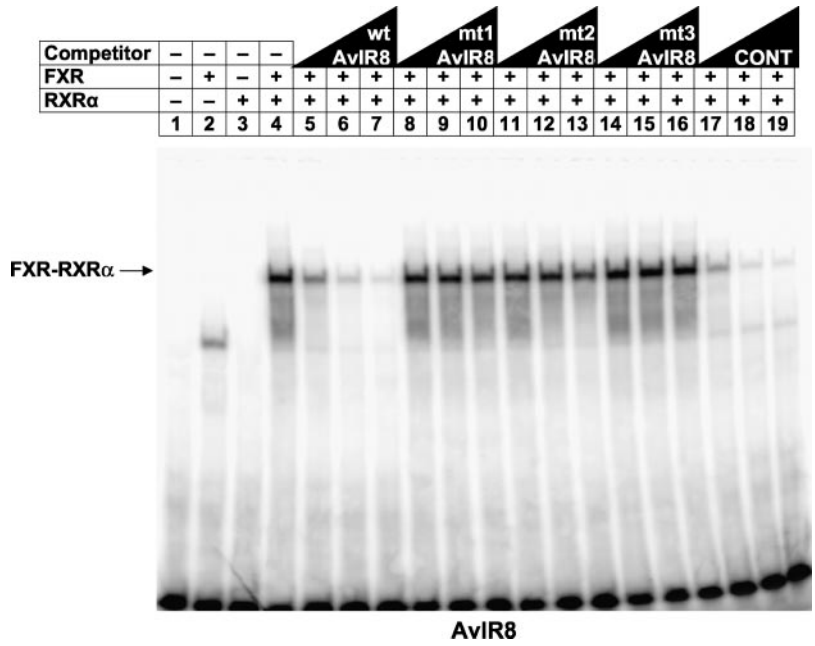

FIG. 11. **The FXR-RXRα heterodimer binds specifically to the IR8 element of the human apoAV promoter.** EMSAs were performed using *in vitro* transcribed/translated human FXR (2.5 μl), human RXRα (2.5 μl), or unprogrammed reticulocyte lysate (−), when indicated, and a labeled double-stranded oligonucleotide corresponding to nt −109 to −80 (*AvIR8*) of the human apoAV gene promoter as described under "Experimental Procedures." The lysate volumes were kept constant by the addition of unprogrammed lysate. The competition experiments for binding of FXR-RXRα heterodimers were performed by adding a 50-, 250-, and 500-fold molar excess of the indicated unlabeled double-stranded probes. The mutations present in the modified versions of *wtAvIR8* (*mt1AvIR8, mt2AvIR8*, and *mt3AvIR8*) are shown in Fig. 10*B*. The specific FXR-RXRα-FXRE complex is indicated by an *arrow*. *CONT*, FXRE of human I-BABP gene (30); *wt*, wild-type; *mt*, mutated.

The FXR-RXRα Heterodimer Binds Specifically to the ApoAV IR8 Element—Direct binding of FXR/RXRα heterodimers to the human apoAV IR8 element was examined. For this purpose, gel shift assays were performed using *in vitro* translated human FXR and RXRα and a radiolabeled double-stranded oligonucleotide containing the apoAV IR8 element. The addition of FXR resulted in the appearance of a weak protein-DNA complex band (Fig. 11, *lane 2*), a phenomenon that we also perceived in previously published gel shift analysis performed with other FXREs (Fig. 5*B* in Ref. 23, Fig. 3*B* in Ref. 29, and Fig. 5*A* in Ref. 30). Nevertheless, this faint band disappeared, and a robust and more shifted band emerged when both FXR and RXRα were present (Fig. 11, *lane 4*). This RXRα-FXR-IR8 binding was specific, as demonstrated by competition of an excess of either unlabeled wild-type apoAV IR8 oligonucleotide (Fig. 11, *lanes 5–7*) or a cold probe containing the IR1 sequence of the human I-BABP FXRE (Fig. 11, *lanes 17–19*). Furthermore, mutation of either half-site (Fig. 10*B*) abolished the ability of the probe to compete (Fig. 11, *lanes 8–16*). These results demonstrate that FXR-RXRα heterodimers are able to directly and specifically interact with the apoAV IR8 and not with cryptic binding motifs embedded within this site. We conclude that this novel IR8 is a *bona fide* FXR response element.

ApoAV mRNA Levels Are Not Induced by Treatments with a FXR Agonist or a Bile Acid—To analyze whether apoAV mRNA expression is regulated by FXR agonists and bile acids, primary hepatocytes isolated from cynomolgus liver and human hepatoma HepG2 cells were incubated for 48 h in medium containing GW4064, LCA, or vehicle. Whereas the treatment of hepatocytes with the FXR agonist or LCA increased the expression of small heterodimer partner and bile salt export pump genes, no significant induction of apoAV expression was observed (Fig. 12).

DISCUSSION

The present study aimed to comprehend the mechanisms controlling the human apoAV gene expression and to identify factors capable of positively modulating its transcription. Our data reveal that two nuclear receptors involved in the regulation of triglyceride metabolism, namely PPARα and FXR, may control the human apoAV gene.

The apoAV gene resides ~27 kb distal to apoAIV in the apoAI/CIII/AIV gene cluster on human chromosome 11q23 (38, 39). Our results showed that the human apoAV gene contains four exons, with the first intron within the 5′-untranslated regions (Fig. 1*A*). With the exception of apoAIV (50), both features are also present in the rest of the apolipoprotein genes (Fig. 1*B*). This similarity gives further insight into the understanding of the process of evolution of the apolipoprotein genes from a common ancestor (51). In addition to the previously reported alternative 3′-untranslated regions (39), we found that the second exon may have alternative length depending on the use of two distinct acceptor sites. Interestingly, alternative transcripts have not been reported for other members within this gene cluster. However, although some variation in terms of mRNA stability may be inferred, none of the alternative transcripts contains a different coding sequence. Strikingly, we came across an SNP (A→G) 3 nt upstream from the predicted translation start codon (Fig. 1*C*). The incidence of this SNP (called c.−3A→G) and its association with higher triglyceride levels were recently reported (42). There is another ATG in frame 9 nt downstream of the start codon (Fig. 1*C*). The nucleotide sequences surrounding both methionine codons conform to the Kozak consensus sequence (RNNATGG), with a G at +4 and a purine (R), preferably A, 3 nucleotides upstream (52). It remains as an interesting question for future research to determine whether this c.−3A→G polymorphism could modify the start of translation or reduce the rate of apoAV protein synthesis. On the other hand, a T→C SNP in the 5′-region of the human apoAV gene, called SNP3, has also been associated with elevated plasma triglyceride levels (38, 41–45). Luciferase reporter assays revealed that the change of the common allele T to C, which is located at position −600 relative to the transcription start site (Fig. 1*C*), has no significant effect on the basal activity of the apoAV promoter. Similarly, the induction by either PPARα or FXR of the apoAV promoter activity was not affected by this change of T to C (data not shown). Analysis of the sequence surrounding SNP3 reveals no apparent transcription factor binding sites. In addition, EMSA showed no binding of nuclear receptors to this region (Fig. 5*A* and data not shown). Considered together, these data suggest that this polymorphism may not be functional but, as proposed by others (43), may act as a marker for another functional change elsewhere in the gene cluster.

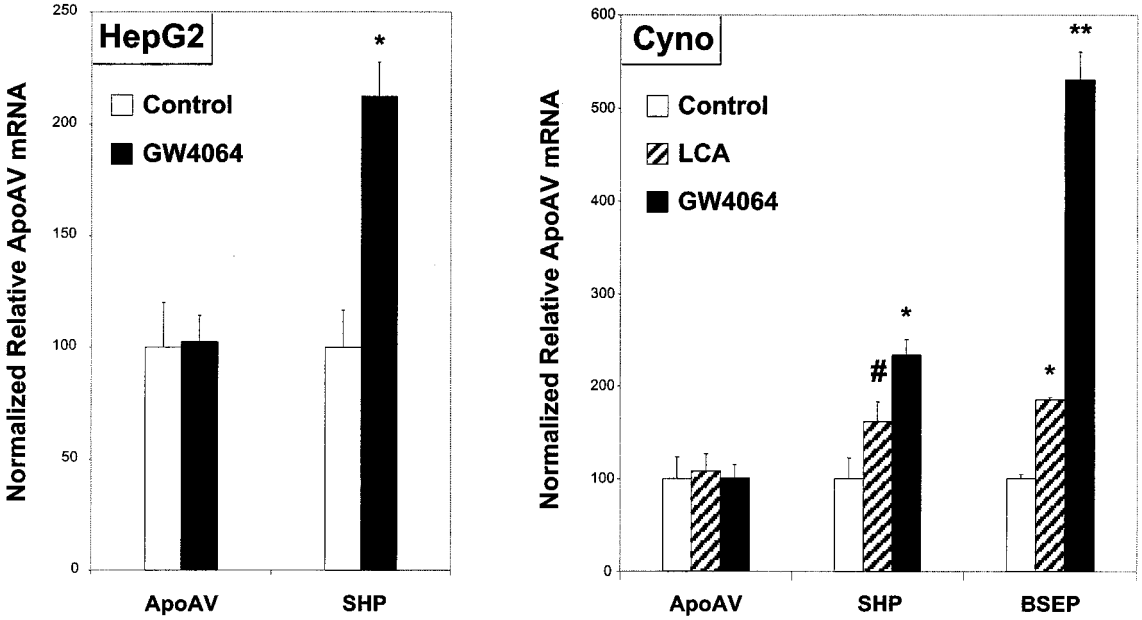

FIG. 12. **apoAV mRNA levels are not induced by treatments with an FXR agonist or a bile acid.** Hepatocytes isolated from cynomolgus liver (*Cyno*) and human hepatoma HepG2 cells were treated for 48 h with vehicle (*Control*), 1 μM GW4064 or 30 μM LCA. Total RNA was extracted for analysis by real time RT-PCR as described under "Experimental Procedures." Specific mRNA levels normalized to 18 S content are expressed relative to untreated cells set as 100 for each gene (mean ± S.D.). Significant differences compared with the untreated control are as follows: *, $p < 0.005$; #, $p < 0.01$; **, $p < 0.0001$.

The presence of a TATA box 30 nt upstream of the start of transcription identified by RLM-RACE along with the results from reporter experiments showing transcriptional activity and responsiveness to nuclear receptors validate this proximal 5′-flanking region as the promoter of the human apoAV gene. The expression of apoAI, apoCIII, and apoAIV is controlled by a common enhancer sequence located at the distal regulatory region of the apoCIII gene (53). Based on the notion that apoAV and these apolipoprotein genes evolved from a common ancestral gene, it is tempting to speculate that a distal enhancer also regulates the apoAV gene. If this is the case, however, then the enhancer for apoAV should be elsewhere within a 26-kb *Xho*I fragment that contains only apoAV, which was able to induce specific expression of human apoAV when injected into mouse eggs (38). Further work will be required to fully assess this hypothesis.

Deletion, site-directed mutagenesis, and binding analysis demonstrated unequivocally that the apoAV gene promoter responds to bile acids and FXR via a novel response element (IR8). Furthermore, the IR8 element was capable of conferring FXR responsiveness on a heterologous promoter in a copy number-dependent manner, and selective mutation of each half-site in the IR8 abolished the nuclear receptor response. However, despite exhaustive efforts, we have not been able to demonstrate a significant induction of apoAV mRNA levels by either bile acids or the FXR ligand GW4064 in hepatocytes (Fig. 12). This paradox suggests that other factors might potentially interfere in the regulation by FXR. Recent studies are beginning to establish the notion that the DNA sequences of hormone response elements for several nuclear receptors, once thought to be specific, can be quite varied. The MRP2 ER8, for example, has been shown to function as a pregnane X receptor (NR1I2), constitutive androstane receptor (NR1I3), and FXR response element (23). It is possible that the novel IR8 could also act as response element for the convergence of alternative transcription factors present in the systems that we have analyzed, and the response to bile acids depends on the ratio between FXR and these factors. Alternatively, sequences in the 5′-flanking region of human apoAV upstream to position −2455 might respond negatively to bile acids and thereby counteract the effect through the proximal FXRE. Further studies will be necessary to determine whether potential activation of the apoAV gene by bile acids is dependent on a particular environmental or physiological cue.

The current study shows that treatment of hepatocytes with a PPARα activator increased apoAV mRNA levels. Consistent with this observation, induction of apoAV mRNA levels by fibrates has recently been reported (54). Furthermore, cotransfection of a PPARα expression plasmid induced the activity of the human apoAV promoter, suggesting that the increase by PPARα activators occurs, at least in part, via transcriptional mechanisms. Using 5′-deletion, mutagenesis, and gel shift analysis, a functional PPRE was identified. A reporter construct bearing a mutated version of this PPRE still showed a minimal transactivation by PPARα. The basis for this residual response is unclear, and the presence of an additional, weak response element between nt −617 and −271 should not be excluded.

It is well established that PPARα activators lower plasma triglyceride levels by modulating the transcription of several lipid-related genes (10). PPARα induces the expression of enzymes involved in the uptake, transport, and metabolism of fatty acids. As a result, the substrate availability for triglyceride synthesis and very low density lipoprotein production is diminished, which will ultimately decrease plasma triglyceride-rich lipoprotein concentrations (11). In addition, activated PPARα may increase LPL-mediated lipolysis and clearance of triglyceride-rich lipoprotein particles by stimulating LPL expression in the liver and by reducing hepatic production of apoCIII (12–15). Our results demonstrate that apoAV is *de facto* a PPARα target gene, which is consistent with the triglyceride-lowering role proposed for apoAV. These findings shed new light on the mechanisms whereby PPARα agonists lower plasma triglyceride levels.

Acknowledgments—We thank J. Kirilovsky and M. Walker for encouragement of this work; D. Grillot and P. Martres for scientific discussions; J. Pilot, V. Baudet, and G. Krysa for technical assistance;

P. A. Wilson for bioinformatics analysis; E. Nicodeme for help with cynomolgus hepatocytes; J. Chapman (U551 INSERM, France) for critical reading of the manuscript; and A. Brewster for manuscript corrections.

REFERENCES

1. Cullen, P. (2000) *Am. J. Cardiol.* **86,** 943–949
2. Jeppesen, J., Hein, H. O., Suadicani, P., and Gyntelberg, F. (1998) *Circulation* **97,** 1029–1036
3. Miller, M., Seidler, A., Moalemi, A., and Pearson, T. A. (1998) *J. Am. Coll. Cardiol.* **31,** 1252–1257
4. Assmann, G., Schulte, H., and von Eckardstein, A. (1996) *Am. J. Cardiol.* **77,** 1179–1184
5. Stampfer, M. J., Krauss, R. M., Ma, J., Blanche, P. J., Holl, L. G., Sacks, F. M., and Hennekens, C. H. (1996) *JAMA* (*J. Am. Med. Assoc.*) **276,** 882–888
6. Fruchart, J. C., and Duriez, P. (2002) *Curr. Opin. Lipidol.* **13,** 605–616
7. Staels, B., Dallongeville, J., Auwerx, J., Schoonjans, K., Leitersdorf, E., and Fruchart, J. C. (1998) *Circulation* **98,** 2088–2093
8. Kersten, S., Desvergne, B., and Wahli, W. (2000) *Nature* **405,** 421–424
9. Issemann, I., and Green, S. (1990) *Nature* **347,** 645–650
10. Desvergne, B., and Wahli, W. (1999) *Endocr. Rev.* **20,** 649–688
11. Barbier, O., Torra, I. P., Duguay, Y., Blanquart, C., Fruchart, J. C., Glineur, C., and Staels, B. (2002) *Arterioscler. Thromb. Vasc. Biol.* **22,** 717–726
12. Winegar, D. A., Brown, P. J., Wilkison, W. O., Lewis, M. C., Ott, R. J., Tong, W. Q., Brown, H. R., Lehmann, J. M., Kliewer, S. A., Plunket, K. D., Way, J. M., Bodkin, N. L., and Hansen, B. C. (2001) *J. Lipid Res.* **42,** 1543–1551
13. Hertz, R., Bishara-Shieban, J., and Bar-Tana, J. (1995) *J. Biol. Chem.* **270,** 13470–13475
14. Staels, B., Vu-Dac, N., Kosykh, V. A., Saladin, R., Fruchart, J. C., Dallongeville, J., and Auwerx, J. (1995) *J. Clin. Invest.* **95,** 705–712
15. Schoonjans, K., Peinado-Onsurbe, J., Lefebvre, A. M., Heyman, R. A., Briggs, M., Deeb, S., Staels, B., and Auwerx, J. (1996) *EMBO J.* **15,** 5336–5348
16. Edwards, P. A., Kast, H. R., and Anisfeld, A. M. (2002) *J. Lipid Res.* **43,** 2–12
17. Forman, B. M., Goode, E., Chen, J., Oro, A. E., Bradley, D. J., Perlmann, T., Noonan, D. J., Burka, L. T., McMorris, T., Lamph, W. W., Evans, R. M., and Weinberger, C. (1995) *Cell* **81,** 687–693
18. Lu, T. T., Repa, J. J., and Mangelsdorf, D. J. (2001) *J. Biol. Chem.* **276,** 37735–37738
19. Makishima, M., Okamoto, A. Y., Repa, J. J., Tu, H., Learned, R. M., Luk, A., Hull, M. V., Lustig, K. D., Mangelsdorf, D. J., and Shan, B. (1999) *Science* **284,** 1362–1365
20. Parks, D. J., Blanchard, S. G., Bledsoe, R. K., Chandra, G., Consler, T. G., Kliewer, S. A., Stimmel, J. B., Willson, T. M., Zavacki, A. M., Moore, D. D., and Lehmann, J. M. (1999) *Science* **284,** 1365–1368
21. Wang, H., Chen, J., Hollister, K., Sowers, L. C., and Forman, B. M. (1999) *Mol. Cell* **3,** 543–553
22. Song, C. S., Echchgadda, I., Baek, B. S., Ahn, S. C., Oh, T., Roy, A. K., and Chatterjee, B. (2001) *J. Biol. Chem.* **276,** 42549–42556
23. Kast, H. R., Goodwin, B., Tarr, P. T., Jones, S. A., Anisfeld, A. M., Stoltz, C. M., Tontonoz, P., Kliewer, S., Willson, T. M., and Edwards, P. A. (2002) *J. Biol. Chem.* **277,** 2908–2915
24. Russell, D. W. (1999) *Cell* **97,** 539–542
25. Chawla, A., Saez, E., and Evans, R. M. (2000) *Cell* **103,** 1–4
26. Chiang, J. Y., Kimmel, R., Weinberger, C., and Stroup, D. (2000) *J. Biol. Chem.* **275,** 10918–10924
27. Davis, R. A., Miyake, J. H., Hui, T. Y., and Spann, N. J. (2002) *J. Lipid Res.* **43,** 533–543
28. del Castillo-Olivares, A., and Gil, G. (2001) *Nucleic Acids Res.* **29,** 4035–4042
29. Ananthanarayanan, M., Balasubramanian, N., Makishima, M., Mangelsdorf, D. J., and Suchy, F. J. (2001) *J. Biol. Chem.* **276,** 28857–28865
30. Grober, J., Zaghini, I., Fujii, H., Jones, S. A., Kliewer, S. A., Willson, T. M., Ono, T., and Besnard, P. (1999) *J. Biol. Chem.* **274,** 29749–29754
31. Laffitte, B. A., Kast, H. R., Nguyen, C. M., Zavacki, A. M., Moore, D. D., and Edwards, P. A. (2000) *J. Biol. Chem.* **275,** 10638–10647
32. Urizar, N. L., Dowhan, D. H., and Moore, D. D. (2000) *J. Biol. Chem.* **275,** 39313–39317
33. Claudel, T., Sturm, E., Duez, H., Torra, I. P., Sirvent, A., Kosykh, V., Fruchart, J. C., Dallongeville, J., Hum D. W., Kuipers, F., and Staels, B. (2002) *J. Clin. Invest.* **109,** 961–971
34. Maloney, P. R., Parks, D. J., Haffner, C. D., Fivush, A. M., Chandra, G., Plunket, K. D., Creech, K. L., Moore, L. B., Wilson, J. G., Lewis, M. C., Jones, S. A., and Willson, T. M. (2000) *J. Med. Chem.* **43,** 2971–2974
35. Kast, H. R., Nguyen, C. M., Sinal, C. J., Jones, S. A., Laffitte, B. A., Reue, K., Gonzalez, F. J., Willson, T. M., and Edwards, P. A. (2001) *Mol. Endocrinol.* **15,** 1720–1728
36. Sinal, C. J., Tohkin, M., Miyata, M., Ward, J. M., Lambert, G., and Gonzalez, F. J. (2000) *Cell* **102,** 731–744
37. Iser, J. H., and Sali, A. (1981) *Drugs* **21,** 90–119
38. Pennacchio, L. A., Olivier, M., Hubacek, J. A., Cohen, J. C., Cox, D. R., Fruchart, J. C., Krauss, R. M., and Rubin, E. M. (2001) *Science* **294,** 169–173
39. van der Vliet, H. N., Sammels, M. G., Leegwater, A. C., Levels, J. H., Reitsma, P. H., Boers, W., and Chamuleau, R. A. (2001) *J. Biol. Chem.* **276,** 44512–44520
40. van der Vliet, H. N., Schaap, F. G., Levels, J. H., Ottenhoff, R., Looije, N., Wesseling, J. G., Groen, A. K., and Chamuleau, R. A. (2002) *Biochem. Biophys. Res. Commun.* **295,** 1156–1159
41. Ribalta, J., Figuera, L., Fernandez-Ballart, J., Vilella, E., Castro Cabezas, M., Masana, L., and Joven, J. (2002) *Clin. Chem.* **48,** 1597–1600
42. Pennacchio, L. A., Olivier, M., Hubacek, J. A., Krauss, R. M., Rubin, E. M., and Cohen, J. C. (2002) *Hum. Mol. Genet.* **11,** 3031–3038
43. Talmud, P. J., Hawe, E., Martin, S., Olivier, M., Miller, G. J., Rubin, E. M., Pennacchio, L. A., and Humphries, S. E. (2002) *Hum. Mol. Genet.* **11,** 3039–3046
44. Endo, K., Yanagi, H., Araki, J., Hirano, C., Yamakawa-Kobayashi, K., and Tomura, S. (2002) *Hum. Genet.* **111,** 570–572
45. Nabika, T., Nasreen, S., Kobayashi, S., and Masuda, J. (2002) *Atherosclerosis* **165,** 201–204
46. McKnight, S. L. (1982) *Cell* **31,** 355–365
47. Coste, H., and Rodríguez, J. C. (2002) *J. Biol. Chem.* **277,** 27120–27129
48. Rodríguez, J. C., Gil-Gómez, G., Hegardt, F. G., and Haro, D. (1994) *J. Biol. Chem.* **269,** 18767–18772
49. Vu-Dac, N., Chopin-Delannoy, S., Gervois, P., Bonnelye, E., Martin, G., Fruchart, J. C., Laudet, V., and Staels, B. (1998) *J. Biol. Chem.* **273,** 25713–25720
50. Elshourbagy, N. A., Walker, D. W., Paik, Y. K., Boguski, M. S., Freeman, M., Gordon, J. I., and Taylor, J. M. (1987) *J. Biol. Chem.* **262,** 7973–7981
51. Haddad, I. A., Ordovas, J. M., Fitzpatrick, T., and Karathanasis, S. K. (1986) *J. Biol. Chem.* **261,** 13268–13277
52. Kozak, M. (1996) *Mamm. Genome* **7,** 563–574
53. Zannis, V. I., Kan, H. Y., Kritis, A., Zanni, E. E., and Kardassis, D. (2001) *Curr. Opin. Lipidol.* **12,** 181–207
54. Gervois, P., Vu-Dac, N., Jackel, H., Nowak, M., Staels, B., Pennacchio, L. A., Rubin, E. M., Fruchart, J., and Fruchart, J. C. (2002) *Circulation* **106,** 11–301
55. Applied Biosystems (2001) *User Bulletin 2*, Foster City, CA